

System of Control in an Offshore Wind Farm with HVdc Link

MIGUEL MONTILLA-DJESUS*, SANTIAGO ARNALTES** AND DAVID SANTOS MARTIN**

*Universidad de Los Andes-Mérida
Departamento de Potencia
Facultad de Ingeniería, sector La Hechicera
MÉRIDA, VENEZUELA

**Universidad Carlos III de Madrid
Departamento de Ingeniería Eléctrica
Calle Butarque 15, Edif. Betancourt, Leganés,
MADRID, SPAIN

E-Mail: mmiguel@ula.ve , santiago.arnaltes@uc3m.es,
dsmartin@ing.uc3m.es

URL: <http://www.ula.ve>, <http://www.uc3m.es>;

Abstract: -This paper describes the coordination in control systems between the doubly fed induction generator (DFIG) and the firing delay angle control of the rectifier that comprises the HVdc transmission system based on a Line-Commutated Converter; as well as the *Generator + Transmission* topology formed by the DFIG and HVdc-LCC link to maintain the voltage and frequency output of offshore wind farms constant.

Key-Words: - Wind Power Generation, Doubly Fed Induction Generator, HVdc transmission, Control System.

1 Introduction

The main aim of this paper is to model and control an offshore wind farm and its connection through an appropriate underground transmission system. The connection can be either High Voltage ac (HVac) or High Voltage dc (HVdc). However and due to the ac cables existing limitations for distances above approximately 30km [1],[2], it may be necessary to use the HVdc link. The application of this system to offshore wind farms of the future will allow for transmission distances of more than 100km and will produce transmitted powers above 400MW[3],[4],[5]. Hence, the system has the following objectives:

- To model and control the doubly fed induction generator (DFIG), for isolated operation.
- To model and control an HVdc transmission system based on a Line-Commutated Converter (LCC).

When designing and planning the control operations for either the steady state or transient state of the DFIG and the HVdc-LCC link, the following two problems are considered:

- DFIGs are usually connected to the grid. This network generally has small short circuit impedance (strong grid). However, in this study, the DFIG will be connected to a system with short-circuit impedance different from that of a strong grid, i.e. operating in an isolated way. The HVdc transmission system, when connecting itself to the DFIG terminals, will behave as a

passive load that varies according to the power required in the point of common connection (PCC). Thus, one of the main solutions is to redesign a new control system for the DFIG that will regulate the level of voltage and frequency during the changes in the power system, in coordination with the HVdc control.

- A requirement of the HVdc-LCC transmission is that the converters of the system are connected to ac sources with well-regulated voltage and frequency. In this study a new connection type is implemented for the HVdc-LCC. One of its aims will be an isolated system in which imbalance of the real and reactive power during a transient may cause variations in the voltage and frequency. Hence the study redraws the control of the HVDC converters to regulate the frequency and to transmit the power required by the changes that the load imposes.

In the literature, the isolated operation of the doubly fed induction generator is presented with the purpose of regulating voltage and frequency in the terminals of the machine [6],[7]. This study maintains this approach (isolated operation), but does not include the control of voltage and frequency, which will be assumed by the HVdc rectifier. The real power (P_g) is determined by the DFIG power tracking algorithm and wind condition. A form of imposing the stator voltage in isolated operation is to explicitly specify the reference stator flux linkage of the controller [7].

On the other hand, the HVdc faces a new control paradigm. The HVdc control principle is to regulate the frequency and voltage of the bus rectifier. The real and reactive power transmitted by the HVdc link, (Pd) and (Qd), are related to the voltage and frequency of this bus. The aim of the HVdc is to regulate the frequency by controlling the firing delay angle of the rectifier.

2 Principles of control

The control action of the DFIG is featured by the variable speed constant frequency mode, where the obtention of maximum power from the wind turbine and a constant frequency connection with the power systems are primary concerns [8]. The point of common connection (PCC) imposes the frequency and magnitude of the stator voltage in the generator, and depending on whether the network is weak or strong, it will remain constant during the operation periods of the generator. The controller in the rotor depends on the stator voltage. If the DFIG is connected to a HVdc link, it will not provide a stiff ac voltage source to the control system of the DFIG. It will behave as a passive load that varies the magnitude voltage when the power transmitted changes. In this way, the traditional control of a DFIG [8],[9],[10],[11] is different when the generator is connected to a HVdc link. As the asynchronous generator must now impose the voltage and frequency to the system, it must operate in isolation. The stator voltage and frequency are related approximately as shown below [12],[13]:

$$U_s \approx \omega_1 \psi_s \quad (1)$$

where ψ_s is stator flux, U_s is module phase stator voltage and ω_1 is the grid angular frequency.

The DFIG is controlled in a synchronously rotating dq axis frame, with the d-axis oriented along the stator flux vector position [8],[9],[10],[11]. For this study, the angle of the stator flux is obtained from a QPLL whose input is measured voltage [14]. The QPLL provides an estimation of the frequency. The amplitude and phase angle are not directly estimated by the QPLL but are, however, attainable through calculation procedures. From (1) it is possible to find the stator flux, when the voltage is fixed by the grid. In isolated operation of a DFIG, the stator flux cannot initially be found by equation (1) as there is no stator voltage. One way to solve this issue is to find the suitable variable to control the stator flux within the control system, and to keep the stator voltage constant without taking into account the generator's operation. Therefore, it is necessary that the rotor-

side converter is set at an explicit reference stator flux in order to keep *the stator voltage* constant. Starting from the machine equation in a synchronously rotating dq reference frame with the d-axis aligned along the stator flux vector position, *the control law* will seek to control the stator flux and hence the stator voltage, as follows:

$$-\bar{u}_{ds} = R_s \bar{i}_{ds} + \frac{1}{\omega_{base}} \frac{d\bar{\psi}_{ds}}{dt} - \bar{\psi}_{qs} \quad (2)$$

$$-\bar{u}_{qs} = R_s \bar{i}_{qs} + \frac{1}{\omega_{base}} \frac{d\bar{\psi}_{qs}}{dt} + \bar{\psi}_{ds} \quad (3)$$

$$-\bar{u}_{dr} = R_r \bar{i}_{dr} + \frac{1}{\omega_{base}} \frac{d\bar{\psi}_{dr}}{dt} - s\bar{\psi}_{qr} \quad (4)$$

$$-\bar{u}_{qr} = R_r \bar{i}_{qr} + \frac{1}{\omega_{base}} \frac{d\bar{\psi}_{qr}}{dt} + s\bar{\psi}_{dr} \quad (5)$$

$$\bar{\psi}_{ds} = L_s \bar{i}_{ds} + L_m \bar{i}_{dr} = L_m \bar{i}_{ms} \quad (6)$$

$$\bar{\psi}_{qs} = L_s \bar{i}_{qs} + L_m \bar{i}_{qr} \quad (7)$$

$$\bar{\psi}_{dr} = L_r \bar{i}_{dr} + L_m \bar{i}_{ds} \quad (8)$$

$$\bar{\psi}_{qr} = L_r \bar{i}_{qr} + L_m \bar{i}_{qs} \quad (9)$$

where ψ_{ds} and ψ_{qs} represent the stator flux linkage in synchronous coordinates, ψ_{dr} and ψ_{qr} the rotor flux linkage in synchronous coordinates, u_{ds} and u_{qs} the stator voltage in synchronous coordinates, u_{dr} and u_{qr} the rotor voltage in synchronous coordinates, i_{ds} and i_{qs} the stator current in synchronous coordinates, i_{dr} and i_{qr} the rotor in synchronous coordinates, s the slip and ω_{base} the base frequency. The parameters of the machine R_s , R_r , L_s , L_r and L_m represent the stator resistance, rotor resistance, stator inductance, rotor inductance and mutual inductance, respectively.

Under stator flux vector, $\bar{\psi}_s$, orientation, the component in the q-axis is equal to zero ($\psi_{ds}=0$). Therefore the variable to control the stator flux is the magnetizing current (i_{ms}) through i_{dr} . From (6), the following can be obtained:

$$\bar{i}_{qr} = -\frac{L_s}{L_m} \bar{i}_{qs} \quad (10)$$

Using (10), (5), (7), (8) and (9) in (2) and (3):

$$\frac{L_s}{R_s} \frac{1}{\omega_{base}} \frac{d\bar{i}_{ms}}{dt} + \bar{i}_{ms} = \bar{i}_{dr} - \frac{1+s}{R_s} \bar{u}_{ds} \quad (11)$$

$$\frac{L_s}{R_s} \dot{i}_{ms} = \dot{i}_{qr} - \frac{1 + \sigma_s}{R_s} u_{qs} \quad (12)$$

where $\sigma_s = \frac{L_s - L_m}{L_m}$ is the stator leakage factor.

In (11), i_{ms} can be controlled through i_{dr} . The influence of u_{ds} is small and can be viewed as a disturbance within the control action in the rotor controller [7]. Fig. 1 shows the control loop for the magnetizing current.

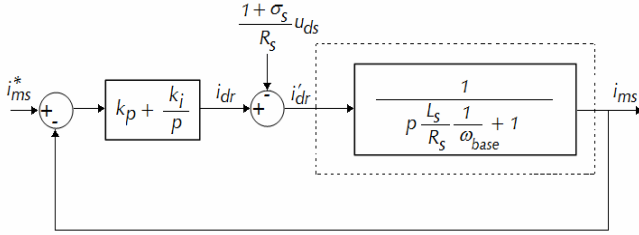


Fig.1: Block diagram of the magnetizing current control systems.

The stator flux is established by the magnetizing current instead of by the stator voltage, as there is initially no stator voltage in isolated operation. The vector control schematic of the DFIG is shown in Fig. 2.

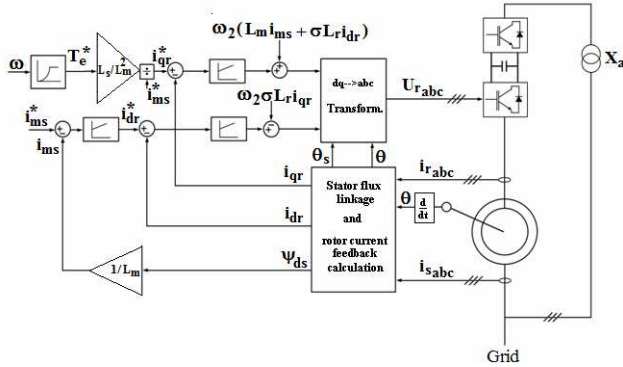


Fig.2: Control scheme of the DFIG in isolated operation.

2.1 Analysis of the isolated operation of a DFIG

This subsection investigates the performance of the DFIG in isolated operation. The frequency depends on the characteristics of load and on the control characteristics of the DFIG [13]. For a given wind speed, the real output power of the generator is known. This value is denoted as P_g . With this power, and considering the stator flux ψ_s , the stator voltage and frequency can be decided with the load characteristic as expressed for a series R and L static load. The real and reactive single power of the load can be written in terms of voltage and frequency as:

$$P_g = \frac{U_s^2}{R^2 + (\omega_s L)^2} R \quad (13)$$

$$Q_g = \frac{U_s^2}{R^2 + (\omega_s L)^2} (\omega_s L) \quad (14)$$

Replacing the equation (1) in (13), the frequency and voltage in steady state according to the characteristic load:

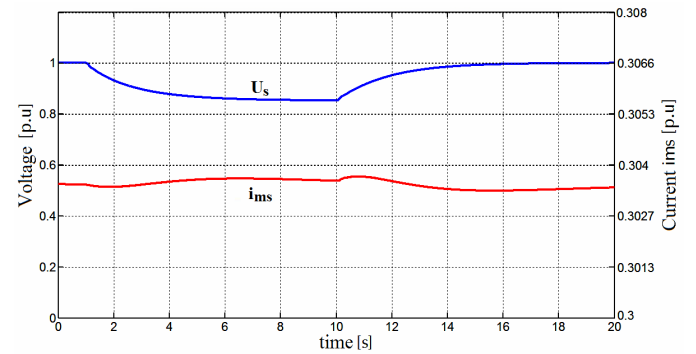
$$\omega_s = \sqrt{\frac{P_g R^2}{\psi_s^2 R + P_g L^2}} \quad (15)$$

$$U_s = \sqrt{\frac{P_g R^2 \psi_s^2}{\psi_s^2 R + P_g L^2}} \quad (16)$$

Unbalances of active or reactive power, for example during a transient, will result in variations for both frequency and voltage. To maintain constant values of frequency and stator voltage, both the stator flux and the power generated by the DFIG must be controlled. In the literature, the isolated operation DFIG is present. This study maintains the same control approach (isolated operation), but does not include voltage and frequency control, which will be assumed by the rectifier of the HVdc. The real power is determined by the DFIG power tracking algorithm and wind condition. The DFIG is simulated in isolated operation, and this supplies an RL load. The passive load is 1.2MVA with a lagging power factor of 0.99. The wind speed incident on the turbine is $v_n = 11.57 \text{ m/s}$. Simulations are carried out for two different scenarios, with changes in wind input and in load impedance, respectively.

2.1.1 Changes in wind speed

A sudden step change (10% reduction) of wind speed is simulated at $t=1\text{s}$, and returns to its initial value at $t=10\text{s}$.



(a)

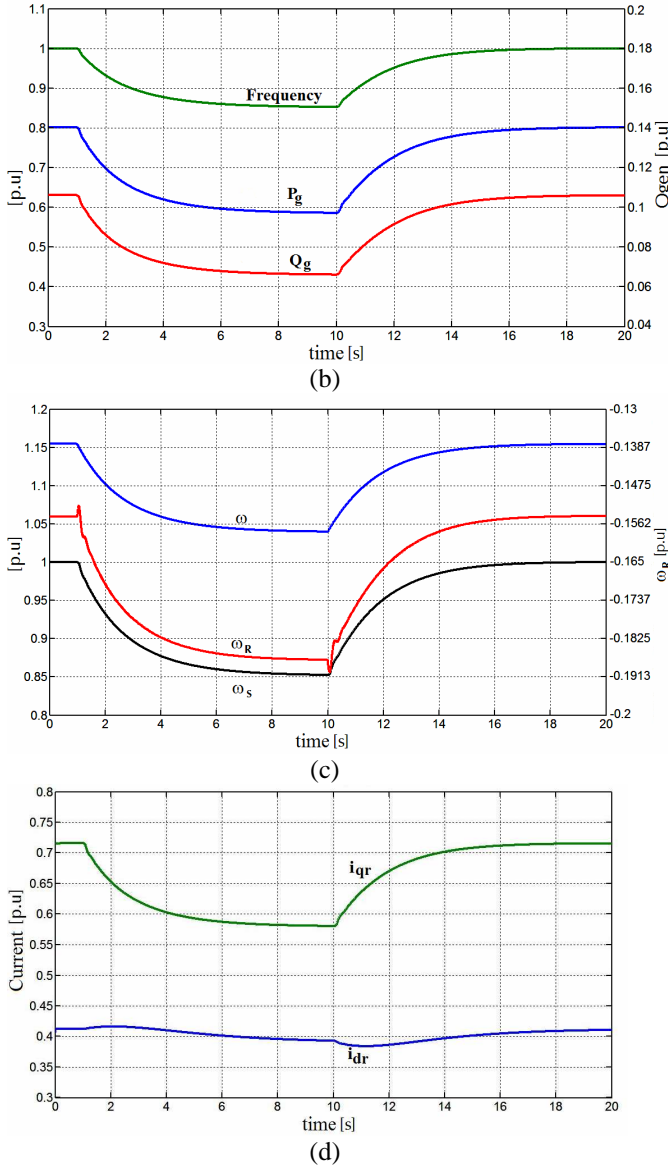


Fig.3. Response of DFIG in isolated operation -wind speed change: (a) stator voltage and magnetizing current (b) generated active and reactive power, Frequency (c) angular frequency stator (ω_s), angular frequency generator rotor (ω_r) and angular frequency sliding (ω) (d) rotor current components.

As shown in Fig. 3a, stator voltage U_s drops from 1pu to 0.85pu. This decrease follows the change in wind speed. Note how the stator voltage is a function of the output power of the DFIG (Fig. 3b). Note also that the control system in the rotor controller follows the change imposed by the wind speed but does not adjust the voltage level at a given reference. The rotor control system sets the stator flux through the magnetizing current (see Fig. 3a). As the angular frequency generator rotor (ω_r) changes due to wind speed, the angular frequency sliding (ω_s) also changes as shown in Fig. 3c in order to fulfill the equation: $\omega_s = \omega + \omega_r$

Finally, Fig 3d shows how rotor current component i_{qr} changes value with respect to the output power. When applying vector control in DFIG, the active and reactive stator power is a function of the rotor current components i_{qr} and i_{dr} . Therefore we have:

$$P_s = \left| \bar{\mathbf{u}}_s \right| \frac{L_m}{L_s} \bar{i}_{qr} \quad (17)$$

$$Q_s = -\left| \bar{\mathbf{u}}_s \right| \frac{L_m}{L_s} (\bar{i}_{ms} - \bar{i}_{dr}) \quad (18)$$

As the active and reactive power balance at the DFIG terminals is equal to:

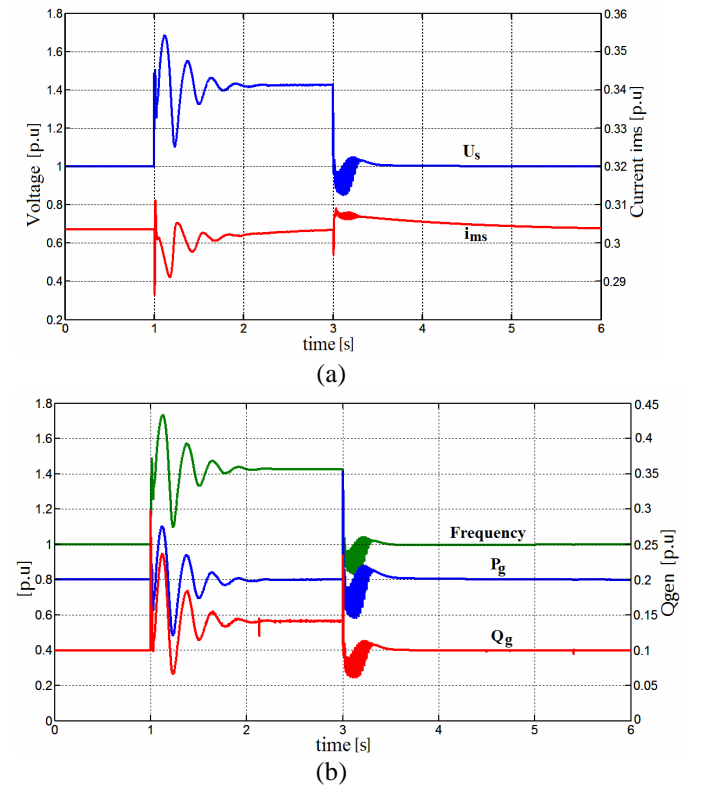
$$P_g = P_s + P_a \quad (19)$$

$$Q_g = Q_s \quad (20)$$

By reducing P_g and U_s , the stator power decreases. Therefore, the rotor current component i_{qr} decreases too.

2.1.2 Changes in passive load

In this second scenario, the load simulated is for a sudden change of load equal to half the initial value at $t=1$ s, to return to its initial value at $t=3$ s.



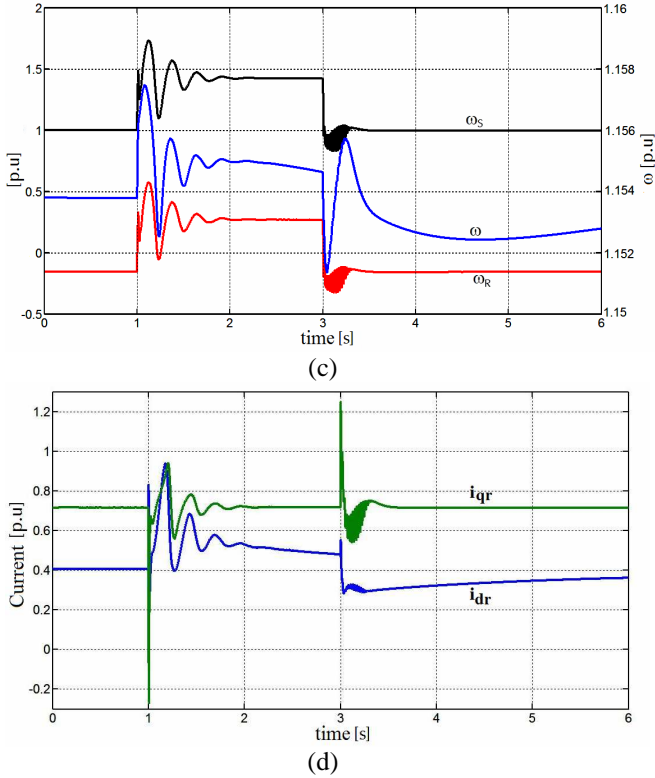


Fig.4. Response of DFIG in isolated operation-load change: (a) stator voltage and magnetizing current (b) generated active and reactive power, Frequency (c) angular frequency stator (ω_s), angular frequency generator rotor (ω) and angular frequency sliding (ω_R) (d) rotor current components.

Figure. 4a shows the stator voltage U_s increase. This increase is mainly due to the change in the load at $t=1s$, and not to the change in output power, which remains constant as shown in Fig 4b. Fig. 4a shows that the magnetizing current (i_{ms}) remain constant. Note in Fig. 4c as the angular frequency generator rotor (ω) is constant throughout the simulation. To satisfy the equation $\omega_s = \omega + \omega_R$, all the change is reflected in the angular frequency sliding (ω_R). The rotor control system tries to compensate for the changes introduced by the load, varying the rotor current, and thus making the output power of the DFIG equal to the load power as seen in Fig. 4d.

3 Control Principle of the High-Voltage direct current (HVdc) Link

This section shows the control system to be performance by the HVdc rectifier. The HVdc has a bipolar configuration with a 12 pulse arrangement that consists of 2 serial bridges per converter station and metallic return, as shown in Fig. 5.

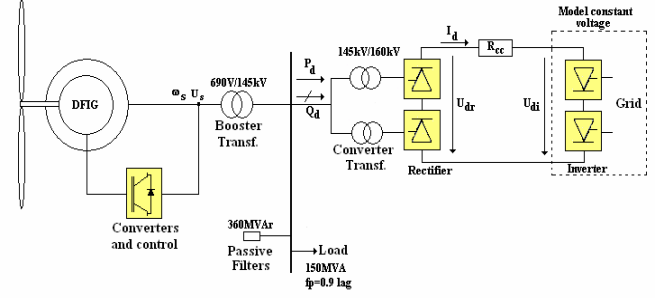


Fig.5: Systems configuration DFIG+HVdc

This model assumes that the inverter will work at a constant voltage. All harmonic voltage and current produced by the converter is filtered by the passive filter in the rectifier bus. In addition, part of the reactive power required for HVdc operation is delivered through passive filters. The control principle of the HVdc is to regulate the frequency and voltage of the bus rectifier. The real and reactive power transmitted by HVdc link, P_d and Q_d , are related to the voltage and frequency in this bus. The aim of the HVdc is to regulate the frequency by controlling the firing delay angle of the rectifier. The flow power, usually adjusted with the firing delay angle of the traditional HVdc, is now adjusted by the DFIG through the characteristic of maximum power tracking and the conditions of the wind.

The equations related to ac- and dc- side variables are shown as:

$$U_{dor} = B \frac{3\sqrt{2}}{\pi} U_{LL} \quad (21)$$

$$R_c = B \frac{3}{\pi} X_c = B \frac{3}{\pi} \omega_s L_c \quad (22)$$

where U_{dor} represents no-load dc voltage, U_{LL} ac line voltage, R_c is commutation resistance, X_c is commutation reactance and ω_s is angular frequency.

From (21) and (22), the current in the dc link between the two voltage terminals in rectifier U_{dr} and inverter U_{di} can be found as follows:

$$U_{dr} = U_{dor} \cos \alpha - R_c I_d \quad (23)$$

$$I_d = \frac{U_{dr} - U_{di}}{R_{cc}} \quad (24)$$

where R_{cc} is the resistance of the cable in HVdc link. Substituting (23) in (24) and solving, we have:

$$I_d = \frac{U_{dor} \cos \alpha - U_{di}}{R_{cc} + R_c} \quad (25)$$

With equations (23), (24) and (25) and the active power on HVdc link, $P_d = U_{dr} I_d$ could be used to determine the firing delay angle needed to maintain

the system frequency in steady state:

$$\cos \alpha = \frac{P_d R_{cc} + P_d 2 \frac{3}{\pi} \omega_s L_c - 2 \frac{3}{\pi} \omega_s L_s U_{di}}{2 \frac{3\sqrt{2}}{\pi} \sqrt{3} \cdot \psi_s \omega_s R_{cc}} \quad (26)$$

The equation (26) shows that if the frequency decreases, the firing delay angle decreases, i.e. the firing instant would then advance [13]. When ac voltage at rectifier bus decreases, the firing delay angle decreases to transmit the same power that was had before the change in voltage. The equation (26) is difficult to measure or estimate. It is therefore not practical to use the equation to determine and to control the firing delay angle of the HVdc rectifier. To do this it is possible to devise a negative feedback control loop for the system frequency, where ω_s is the reference at the system bus bar. Fig. 6 shows the control scheme.

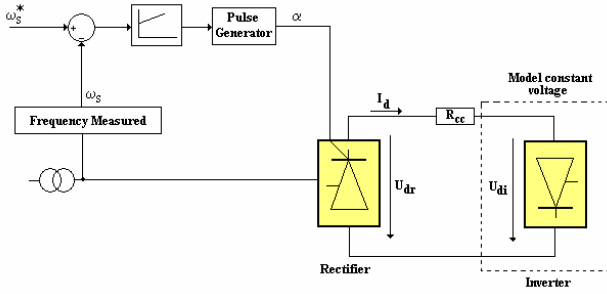


Fig.6. Block diagram of frequency control system in rectifier HVdc.

The HVdc's aim is to maintain constant frequency by controlling the firing delay angle of the rectifier. For a deviation in wind speed, the output real power (P_g) of the DFIG changes following the optimal power tracking control. If the load characteristic stays constant, the stator voltage and frequency vary [13],[14]. At this point the firing delay angle of the rectifier of the HVdc begins to work to regulate the frequency and voltage magnitude at the nominal levels of the machine. The control strategy inside the generator is to maintain stator flux linkage regardless of the change of load or the variations in wind. The response of the coordinated control is quick, because a transitory mechanical does not exist in the process of frequency regulation. Consequently, the power flow in the HVdc link is instantaneous.

4 Case Study

Once the control systems of the DFIG and the HVdc are designed, there will be simulations of the systems to test their coordinated control. The offshore wind farm is an aggregate model which represents the

dynamics of 534 DFIG, each rated at 1.5MW for a nominal capacity of 801MW wind farm. The aggregate model considers all the dynamic characteristics of generators, the coupling systems and the aerodynamic turbines in an equivalent circuit [4]. The representation of these features is essential to avoid introducing errors. The power equations in the aggregate model are:

$$P_g = \sum_{i=1}^N P_i \quad (21)$$

$$Q_g = \sum_{i=1}^N Q_i \quad (22)$$

where N is the wind turbines numbers.

The aggregate model of the offshore wind farm connects the HVdc link through a step-up transformer of 690/145kV. The HVdc link has a rating of 800MW, ± 400 kV bipolar 12-pulse. The rated current of HVdc is 2kA and smoothing inductor 0.3H. The HVdc has two rectifier transformers connected in a delta-star and another star-star, each with 145/160kV. To obtain a sinusoidal waveform to the input of the HVdc link, four passive filters are connected to the rectifier bus with a nominal reactive power of 90MVar each and tuned to the 11^{va}, 13^{va}, 24^{va} y 25^{va} of fundamental frequency. The reactive power demanded by the HVdc is delivered by passive filters. The local load is 150MVA with a power factor of 0.9 lagging. There are two scenarios for the simulation:

- Change in wind speed connection without local load. It considers the following conditions: The wind farm delivers 640MW and 80MVar, the wind speed is 11.57m/s, the wind speed is step decreased by 20% at $t=3$ s and the DFIG at the maximum supersynchronous speed. The wind speed returns to its initial value at $t=12$ s.
- Change in local load. It considers the following conditions: The wind farm delivers 640MW and 80MVar, the wind speed is 11.57m/s, the local load connects at $t=2$ s and the DFIG at the maximum supersynchronous speed. The local load disconnects at $t=3$ s.

5 Simulation Results

5.1 Change in wind speed connection without local load

Figure 7a shows the stator voltage U_s at the offshore wind farm's bus bar. Note how the voltage is unchanged throughout the simulation. When the wind speed decreases so does the power supplied by the wind farm. Fig. 7b shows the active power, reactive power generated and the frequency by the offshore

wind farm. The frequency and magnetizing current is held constant. (See Fig. 7a and 7b). On the other hand, the reactive power generated by the offshore wind farm is increasing in $t=3s$. This is because at that moment, the reactive power demanded by the HVdc cannot be delivered completely through the filters. In Fig. 7c shows that the angular frequency stator is kept constant. To satisfy the equation $\omega_s = \omega + \omega_R$, the only change that occurs in the aggregate model is the angular frequency sliding as shown in Fig. 7c.

Finally, Fig. 7d shows shows rotor current components i_{dr} and i_{qr} . The i_{dr} decreases and so does the reactive power delivered by the wind farm. In the same way changes in i_{qr} are caused by changes in wind speed.

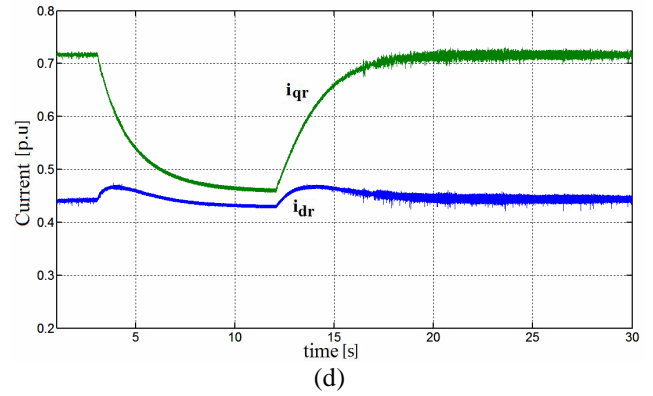
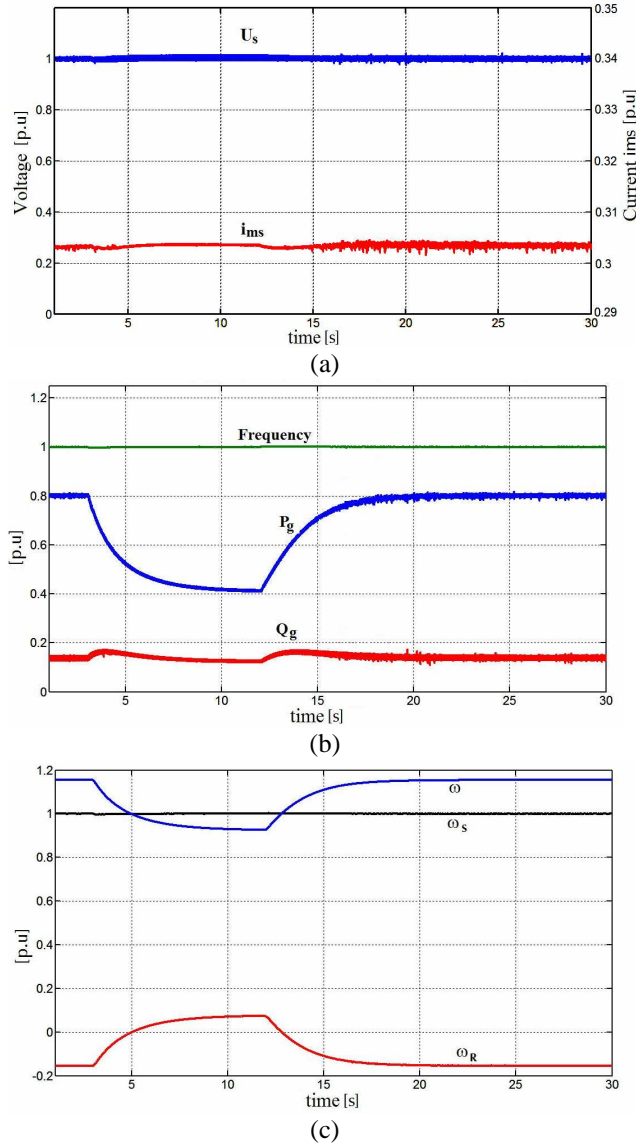
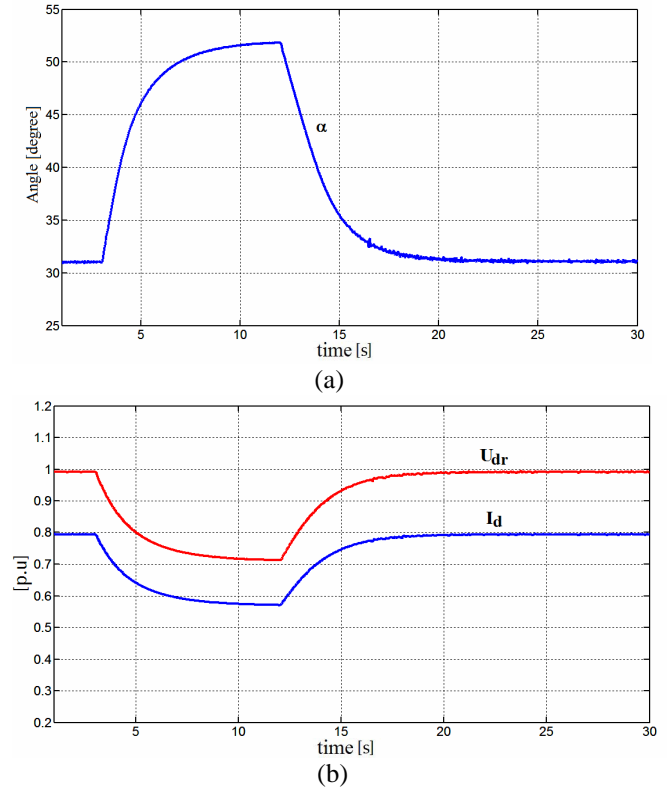


Fig.7. Response of a wind farm with HVdc- wind speed change: (a) stator voltage and magnetizing current (b) generated active and reactive power, Frequency (c) angular frequency stator (ω_s), angular frequency generator rotor (ω) and angular frequency sliding (ω_R) (d) rotor current components.

As shown in Fig. 8, the firing delay angle at the rectifier increases its value in order to maintain the frequency, fallen at $t=3s$, constant. With this change in angle, the dc voltage in the HVdc link decreases to match the power transmitted by the HVdc (Fig.8 b and c).



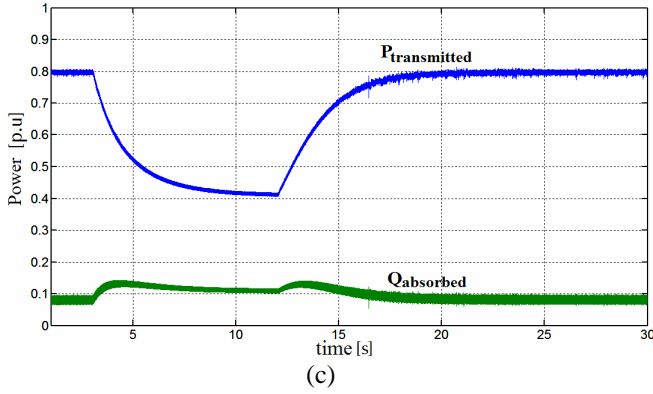


Fig.8. Response of the wind farm with HVdc- wind speed change: (a) firing delay angle at rectifier (b) dc voltage and current at rectifier (c) transmitted active and absorbed reactive power

5.2 Change in local load

In Fig. 9a shows how the stator voltage U_s fall after the disturbance. These recover when the HVdc controller comes into operation. In this figure the magnetizing current is kept constant by the coordinated control. Fig. 9b shows how the active power generated by the wind farm is kept constant after the change in local load. As there is no change in wind speed there is no change in the active power. On the other hand, the frequency falls at $t=2s$ but recovers immediately when the control firing delay angle comes into operation as shown in Fig 9b.

In Fig.9c shows, as in the previous case, the angular frequency stator is kept constant. For this, the equations $\omega_s = \omega + \omega_R$ kept constant at all times and only small oscillations in the angular frequency sliding (ω_R) when there are changes in local load. The angular frequency generator rotor of the aggregate model (ω) remains constant throughout the simulation. Finally, Fig. 9d shows how rotor current component i_{qr} is kept constant due to the lack of change in wind speed.

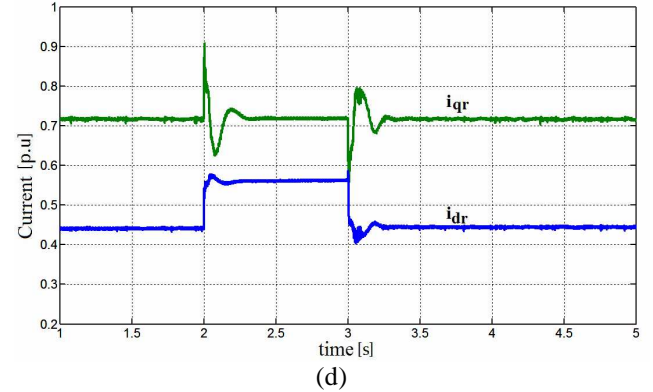
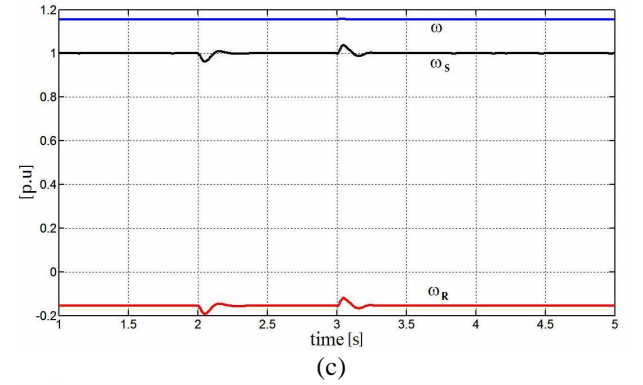
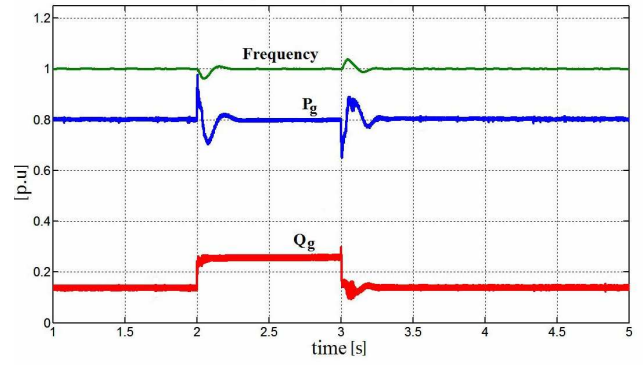
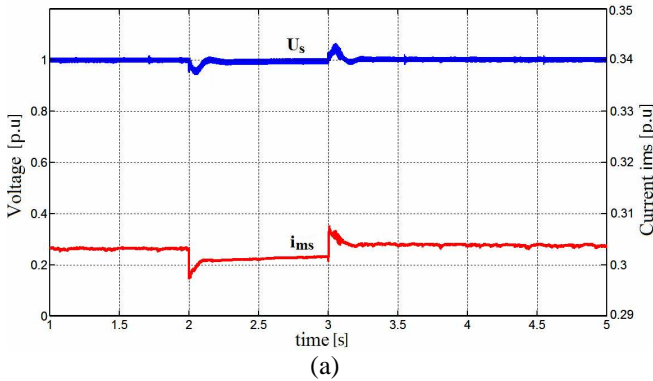


Fig.9. Response of the wind farm with HVDC- local load change: (a) stator voltage and magnetizing current (b) generated active and reactive power, Frequency (c) angular frequency stator (ω_s), angular frequency generator rotor (ω) and angular frequency sliding (ω_R) (d) rotor current components.

In Fig. 10a shows how the firing delay angle changes to compensate the active power at the rectifier bus of the HVdc link. The balance of the active power in the rectifier bus when the local load is applied causes the power transmitted to be lower than the power generated by the wind farm. Therefore, Fig 10b shows the U_{dr} drop in the HVdc link. Fig. 8b shows a change in the reactive power caused by injecting the reactive filters. As the local load is applied, it introduces small reactive power consumption at the rectifier bus and the reactive power absorbed by the HVdc link is about 60% of the nominal active power transmitted. Therefore, there is a difference of more

or less 100MVar in the consumption of the rectifier. This difference increases the reactive power at the HVdc link, as shown in Fig. 10c

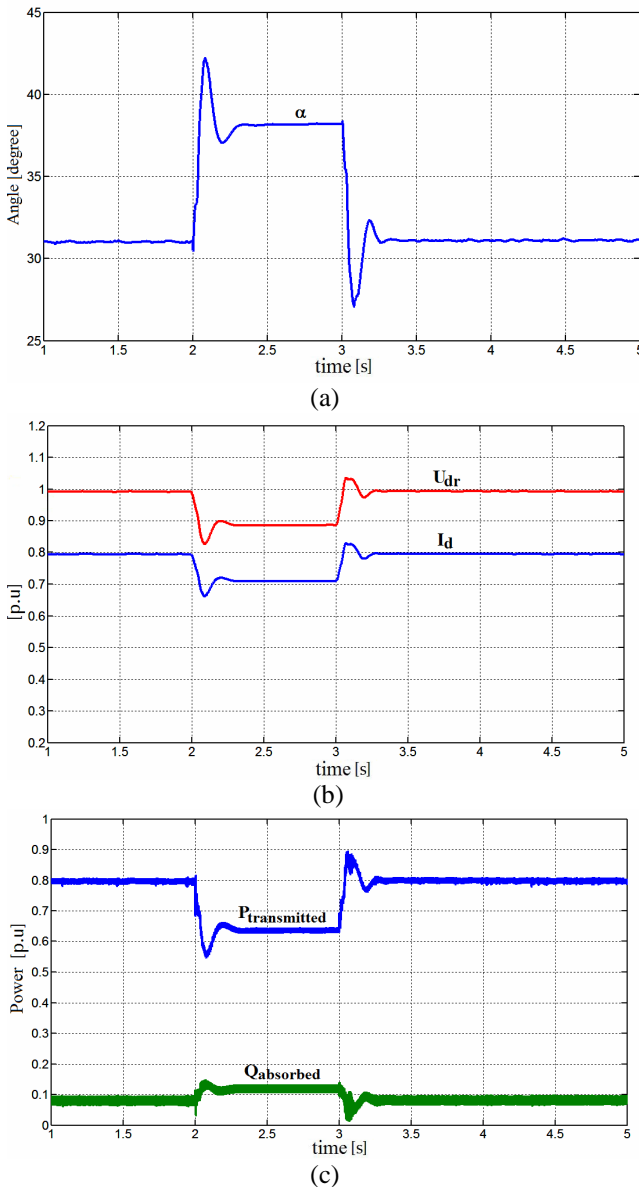


Fig.10. Response of the wind farm with HVdc- local load change: (a) firing delay angle at rectifier (b) dc voltage and current at rectifier (c) transmitted active and absorbed reactive power

4 Conclusion

This paper presents a control method that coordinates doubly fed induction generators (DFIG) with HVdc transmission systems to be used in offshore wind farms. The study and simulations show how the HVdc+DFIG regulate both frequency and voltage before changes in wind speed and disturbance load. The control law is based on using grid frequency control to regulate the firing delay angle of the HVdc rectifier and hence control the power flow to the

system. The power flow, usually adjusted with the firing delay angle in the traditional HVdc, is now adjusted by the DFIG through the characteristic of maximum power tracking and the conditions of the wind. A programmed cubic relation between the output real power and the speed of the rotor is integrated into the control algorithm of the rotor.

References:

- [1]. Stevenson W, "Análisis de Sistemas Eléctricos de Potencia" McGraw-Hill, México, 1988.
- [2]. Gómez Expósito Antonio, "Análisis y operación de sistemas de energía eléctrica" McGraw-Hill, Madrid, 2002.
- [3]. Martander Olof, "DC Grids for Wind Farms" Thesis of Licentiate, School of Electrical and Computer Engineering, Chalmers University of Technology, Göteborg, Sweden 2002.
- [4]. Ackermann T, "Wind Power in Power Systems", John Wiley & Sons, England 2005.
- [5]. Lundberg Stefan, "Configuration Study of Large Wind Park", Thesis of Licentiate, School of Electrical and Computer Engineering, Chalmers University of Technology, Göteborg, Sweden, 2003.
- [6]. Peña Guíñez Ruben, "Vector Control Strategies for a Doubly fed Induction Generator Driven by a Wind Turbine" PhD Thesis, University of Nottingham, UK, 1996.
- [7]. Peña R. Clare J.C., and Asher G.M., "A doubly fed induction generator using back to back PWM converters supplying an isolated Load from a Variable Speed Wind Turbine", IEE Proceeding Electric Power Applications, Vol. 143, No. 5, September 1996.
- [8]. Müller S, Deicke M., and De Doncker R. "Doubly Fed Induction Generator Systems for Wind Turbines", IEEE Industry Applications Magazine, pp. 26-33, May-June 2002.
- [9]. Peña R., Clare J.C., and Ascher G.M., "Doubly Fed Induction Generator using back-back PWM converters and its application to variable-speed wind energy generation" IEE Proceeding Electric Power Applications, Vol. 43, No. 3, pp. 231-241, March 1996.
- [10]. Ekanayake J.B., Holdsworth L, and Jenkins N, "Comparison of 5th order and 3rd order machine models for doubly fed induction generator (DFIG)" Elsevier Electric Power Systems Research, Vol. 67, pp. 207-215, 2003.
- [11]. Hopfensperger B., Atkinson D., and Lakin R.A., "Stator flux oriented control of a doubly fed induction machine with and without position encoder", IEE Proceeding Electric Power

Applications, Vol. 147, No. 4, pp. 241-250, July 2000.

- [12]. Ledesma P, and Usaola J. "Doubly Fed Induction Generator Model for Transients Stability Analysis", IEEE Transactions on Energy Conversion, Vol. 20, No. 2, 388-397 pp., June 2005.
- [13]. Xiang D., Ran L., Bumby J., Tavner P., and Yang S., "Coordinated control of an HVDC Link and Doubly Fed Induction Generation in a Large Offshore Wind Farm", IEEE Transactions on Power Delivery, Vol. 21, No. 1, 463-471 pp., January 2006.
- [14]. Karimi H., Karimi-Ghatermi M., and Iravine M.R., "Estimation of frequency and its rate of change for applications in Power Systems", IEEE Transactions on Power Delivery, Vol. 19, No. 2, April 2004.
- [15]. Li R., Bozhko S., Asher G.M., Clare J.C., Yao Li, and Sasse C. "Grid Frequency Control Design for Offshore Wind Farm with Naturally Commutated HVDC Link Connection", IEEE ISIE Meeting, Montreal, July 2006.